Journal of
Marine Science and Technology

Volume 25 | Issue 5 Article 7

DYNAMIC RELIABILITY ANALYSIS OF THE CRANE SHIP LIFTING LOAD SYSTEM

Xiao-Rong Yang
Military Transportation University, Tianjin, China., Luai-yxr@163.com

Qiu-Ming Gan
Military Transportation University, Tianjin, China.

Yan-Hong Wang
Military Transportation University, Tianjin, China.

Yong-Bo Zhou
Military Transportation University, Tianjin, China.

Follow this and additional works at: https://jmstt.ntou.edu.tw/journal

Recommended Citation
Yang, Xiao-Rong; Gan, Qiu-Ming; Wang, Yan-Hong; and Zhou, Yong-Bo (2017) "DYNAMIC RELIABILITY ANALYSIS OF THE CRANE SHIP LIFTING LOAD SYSTEM," *Journal of Marine Science and Technology*: Vol. 25: Iss. 5, Article 7.
DOI: 10.6119/JMST-017-0621-1
Available at: https://jmstt.ntou.edu.tw/journal/vol25/iss5/7

This Research Article is brought to you for free and open access by Journal of Marine Science and Technology. It has been accepted for inclusion in Journal of Marine Science and Technology by an authorized editor of Journal of Marine Science and Technology.

Journal of Marine Science and Technology, Vol. 25, No. 5, pp. 552-562 (2017)
DOI: 10.6119/JMST-017-0621-1

DYNAMIC RELIABILITY ANALYSIS OF THE CRANE SHIP LIFTING LOAD SYSTEM

Xiao-Rong Yang, Qiu-Ming Gan, Yan-Hong Wang, and Yong-Bo Zhou

Key words: the crane ship lifting load system, nonlinear responses, the random response spectrum, probability statistics, dynamic reliability.

ABSTRACT

In this paper, the probability of a crane ship lifting load system working safely under given conditions is calculated. First, by using Lagrange's equations, we derived the motion equations of the lifting load system, from which the nonlinear responses of the crane ship and the lifting load system under random sea wave load in time domain are achieved. Their maximum are used to calculate the required thresholds of angular displacement according to the given confirmation criteria. By modal analysis, we obtained its random response spectrums, which are analyzed by using probability statistics. The analysis resulted in the variances of the angular displacement and that of the angular velocity. Finally, the variances are used to analyze the dynamic reliability of the lifting load system according to the first-passage failure criterion.

I. INTRODUCTION

1. Development and Present Situation of Dynamic Reliability

In the 1940s, American Scholar Rice (1944) studied the dynamic response of structures and boundary intersecting and found the mathematical expressions and the expected value of the intersection numbers in time range (0, T). From the 1940s to 1960s, the study of dynamic reliability was focused on one degree of freedom linear system under white noise its because, with Markov distribution, its displacement and velocity are stationary Gauss process, which is theoretically easier to analyze.

Afterwards, the dynamic reliability theory of linear system and nonlinear system under non-stationary random excitation was developed. The first-passage problem of stationary Gauss narrow band process was studied with point process method and the Laplace transform of the first-passage probability was derived by Yang and Shinozuka (1971). Iyenger (1973) expanded the probability distribution function of first passage time into Gram-Charliar series and studied the first-passage problem of stationary and non-stationary response. Gasparini (1979) studied the stationary and non-stationary response of multiple degree of freedom system with mode decomposition method and found that the result could be used to calculate the approximate solution of first-passage probability with the Poisson assumption. Roberts (1975) analyzed "internal and external series" and confirmed that the intersection numbers of non-stationary random process and the boundary conform to the Poisson distribution. Roberts (1978a) studied the first-passage problem of nonlinear system with small dumping, and then adopted the energy envelope method to transform the response of one degree of freedom system into one-dimensional Markov process and derived the Fokker-Planck equation which transferable probability density function of the response must conform to (Roberts, 1978b). The weak nonlinear system with small dumping under white noise excitation was studied by Iwan and Spanos (1978). The accuracy of these equivalent linear methods related to one degree of freedom nonlinear system under earthquake excitation was evaluated and the method of setting up the optimal linear system was submitted by Iwan and Gates (1979).

In the past decade, the research work of dynamic reliability mainly focused on engineering application. The dynamic reliability of structures with hysteresis under compound random load was analyzed by Mochio (1989). Mahadevan and Mehta (1993) studied the dynamic reliability of large-scale frame structures with random finite element method. Fritz et al. (1995) studied the dynamic reliability of nonlinear system under random excitation and analyzed its failure probability, lifetime and accumulated damage probability. The discrete Markov process was used to analyze the dynamic reliability under random impact load by Becker et al. (2002). Random orthogonal expansion method and random perturbation finite element method were adopted to calculate the dynamic response of structures with random parameters by Van den Nieuwenhof et al. (2003) and Kaplunov et al. (2005). The dynamic reliability of dams with random parameters under non-stationary seismic excitation was studied with perturbation method by Chaudhuri and Charkraborty (2006).

Paper submitted 11/24/16; revised 05/17/17; accepted 06/21/17. *Author for correspondence: Xiao-Rong Yang (e-mail: luai-yxr@163.com).*
Military Transportation University, Tianjin, China.

2. Achievements of the Crane ShipLifting Load System Research

Crane ships, also known as floating cranes, are widely used in harbor handling, bridge construction, ocean salvage and other ocean engineering work.

Schellin et al. (1991) established the coupled motion equations between the crane ship and the lifted cargo, and discussed their coupled motion in regular waves. Schellin et al. (1991) investigated the motion response of a shear-leg crane ship which is lifting a heavy load in wave groups. The 9-DOF dynamic model incorporated hull motions which were coupled with nonlinear large-angle load swing and an elastic stretch of the hoisting rope assembly. Clauss et al. (1992) analyzed the motion characteristics of large crane barges, ships and SSCVs. Kral et al. (1995) believed that qualitative changes in the dynamic behavior of offshore systems during operation are mainly caused by varying loads, which are caused by fluid-structure interactions and adopting nonlinear models. Balachandran (1999) investigated the planar control and proposed mechanical filter concept. Henry et al. (2001) established a model of the crane load system by using a rigid massless cable and massive point load. The results of the computer simulation were verified by an experiment on a three-degree-of-freedom ship motion simulation platform. Chin et al. (2001) analyzed the dynamic response of a cable-suspended load and obtained the control method with multiple scales. Ellermann et al. (2002) conducted experimental and theoretical studies on the nonlinear dynamic responses of moored crane vessels under regular waves. With damping and response lag involved, Masoud et al. (2004) carried out the research on the response of the crane ship lifting load system. Cha et al. (2010) established the six degrees of freedom motion equations of the lifting load system, and compared its motion responses with that of the three degrees of freedom motion equations. Al-Sweiti et al. (2007) studied the cargo pendulation control of an elastic ship-mounted crane by using Maryland Rigging system. With finite element method, Ren et al. (2008) established a model of a boom and modeled the motion of a lifted cargo as a planar pendulum of point mass, and studied its dynamic response with numerical method. Chen et al. (2011) discussed the motion responses of a large crane ship and the effects of damping coefficient on the responses.

3. Focus of this Study

The above literatures only involve the coupled motion between a crane ship and its lifted cargo, the dynamic response features and the motion control of the lifting load system, without mentioning its dynamic reliability.

As is known, the motion of a crane ship and that of the lifted cargo are coupled. When the motion of the lifted cargo is obvious enough, the motion of a crane ship will be affected, the collision will arise and dynamic intension of the sling will be increased. Patel et al. (1987) found that at the third level sea state when the significant wave height in P-M wave spectrum is 1.0 m-1.6 m, the lifted cargo swings dangerously and the lifting work must be immediately stopped. The world meteorological and oceanic datum show that 35% of JLOTS sea area will reach the third level sea state (Vaughers and Mardiros, 1997). Therefore, we must evaluate the dynamic reliability of the crane ship lifting load system so as to obtain the probability of the lifting load system working safely under the given sea states. In this paper, the dynamic reliability evaluation method of the crane ship lifting load system is explored and the probability of lifting load system working safely under the given sea states is calculated.

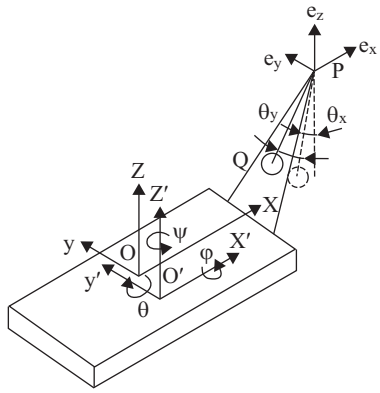

Fig. 1. Coordinate systems.

4. Contents of this Paper

This paper aims to calculate the probability of the crane ship lifting load system working safely in given conditions on the basis of its dynamic responses. In section 2, the motion equations of the lifting load system are derived from Lagrange's equations. In section 3, we introduce the first-passage failure criterion that is used to analyze the dynamic reliability of the lifting load system. In section 4, we give the model and parameters for numerical simulation. In section 5, we analyze random responses of a crane ship and its lifting load system in time domain and frequency domain and calculate the statistical properties of random responses of the crane ship lifting load system with probability statistics, the results of which are used to analyze the dynamic reliability of the lifting load system on the basis of the first-passage failure criterion. Finally, in section 6, is the summary of our study.

II. LIFTING LOAD SYSTEM MOTION EQUATIONS

In this section, the lifting load system motion equations are set up and its motion features are analyzed theoretically.

1. Coordinate Systems

Fig. 1 shows the two coordinate systems which are set up for the purpose of analyzing the lifting load system motions: the inertial coordinate system *o-xyz* fixed on the average position of a crane ship motion and the body-fixed coordinate system *o'-x'y'z'* fixed on a crane ship center of gravity with its *o'x'* axis directing to the ship bow. There are also two angular

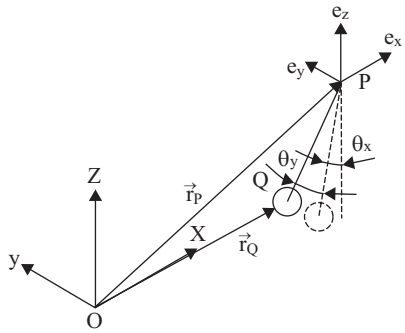

Fig. 2. Coordinates of the lifted cargo in *o-xyz*.

displacements: in-plane angle θ_x and out-plane angle θ_y. In the inertial coordinate system *o-xyz*, θ_x is the included angle between the projection of the sling in *xoz*-plane and *oz* axis and θ_y is the included angle between the sling and *xoz*-plane, which are shown in Fig. 1 The e_x, e_y and e_z in Fig. 1 are unit vectors of the inertial coordinate system *o-xyz* ,which are parallel to *x*, *y*, *z* axis respectively.

2. The Spatial Displacements Expression of the Lifted Cargo

In the body-fixed coordinate system *o'-x'y'z'*, the coordinates of any point *A* are $\begin{bmatrix} x'_A & y'_A & z'_A \end{bmatrix}$. Then the coordinates of the point *A* in inertial coordinate system *o-xyz* can be expressed as:

$$\begin{bmatrix} x_A & y_A & z_A \end{bmatrix}^T = \begin{bmatrix} x_G & y_G & z_G \end{bmatrix}^T + \mathbf{T_o} \cdot \begin{bmatrix} x'_A & y'_A & z'_A \end{bmatrix}^T \quad (1)$$

In Eq. (1), $\begin{bmatrix} x_G & y_G & z_G \end{bmatrix}$ are the coordinates of the crane ship center of gravity in inertial coordinate system *o-xyz*. $\mathbf{T_O}$ is the coordinate transform matrix that can be expressed as the following:

$$\mathbf{T_o} = \begin{bmatrix} 1 & -\psi & \theta \\ \psi & 1 & -\phi \\ -\theta & \phi & 1 \end{bmatrix} \quad (2)$$

In Eq. (2), ϕ, θ, ψ are the angles of the body-fixed coordinate system *o'-x'y'z'* rotating around *x*, *y*, *z* axis respectively.

In Fig. 2, the $\vec{r}_P$ and $\vec{r}_Q$ are the space position vectors of the hanging point *P* and the lifted cargo *Q* in the inertial coordinate system respectively. If the coordinates of the hanging point *P* are $(x_{p'}, y_{p'}, z_{p'})$ in the body-fixed coordinate system, its displacement, speed and acceleration in the inertial coordinates system are as follows based on Eq. (1) (Harnett, 2000).

$$\begin{cases} [x_p\, y_p\, z_p]^T = [x_G\, y_G\, z_G]^T + \mathbf{T_o}[x_{p'}\, y_{p'}\, z_{p'}] \\ [\dot{x}_p\, \dot{y}_p\, \dot{z}_p]^T = [\dot{x}_G\, \dot{y}_G\, \dot{z}_G]^T + \dot{\mathbf{T}}_\mathbf{o}[x_{p'}\, y_{p'}\, z_{p'}] \\ [\ddot{x}_p\, \ddot{y}_p\, \ddot{z}_p]^T = [\ddot{x}_G\, \ddot{y}_G\, \ddot{z}_G]^T + \ddot{\mathbf{T}}_\mathbf{o}[x_{p'}\, y_{p'}\, z_{p'}] \end{cases} \quad (3)$$

In Eq. (3), $\mathbf{T_O}$ is the coordinate transform matrix.

The spatial displacements of the lifted cargo *Q* in the inertial coordinate system can be expressed by Eq. (4).

$$\begin{cases} x_q = x_p - l(t)\sin\theta_x \cos\theta_y \\ y_q = y_p + l(t)\sin\theta_y \\ z_q = z_p - l(t)\cos\theta_x \cos\theta_y \end{cases} \quad (4)$$

In Eq. (4), the sling length *l*, in-plane angle θ_x and out-plane angle θ_y, which are defined in part 2.1, are used to describe the motion of the lifting load system. $\begin{bmatrix} x_q, y_q, z_q \end{bmatrix}$ are also the coordinates of the lifted cargo *Q* in the inertial coordinate system.

3. Motion Equations of the Lifting Load System

The motion equations of the lifting load system can be derived from Lagrange equation which is expressed by Eq. (5) (Li, 2002).

$$\frac{d}{dt}\left(\frac{\partial T}{\partial \dot{q}_i}\right) - \frac{\partial T}{\partial q_i} + \frac{\partial V}{\partial q_i} = Q_i \quad (5)$$

The kinetic energy of the lifting load system is:

$$T = \frac{1}{2}m\dot{x}_q^2(t) + \frac{1}{2}m\dot{y}_q^2(t) + \frac{1}{2}m\dot{z}_q^2(t) \quad (6)$$

In Eq. (6), m is the mass of the lifted cargo and $\begin{bmatrix} x_q, y_q, z_q \end{bmatrix}$ that are expressed by Eq. (4) are the coordinates of the lifted cargo *Q* in the inertial coordinate system.

When the *xoy* plane is regarded as zero potential energy plane, the potential energy of lifting load system is

$$V = mgz_q(t) = mg[z_p(t) - l(t)\cos\theta_x(t)\cos\theta_y(t)] \quad (7)$$

In Eq. (7), *g* is the acceleration of gravity. Eq. (7) is based on Eq. (4).

Substituting Eq. (6), Eq. (7) for the T and V in the Eq. (5), setting $q_1 = x_P$, $q_2 = y_P$, $q_3 = z_P$ in Eq. (5) and adopting the relationship in Eq. (4), we can have the second-order differential equations about in-plane θ_x and out-plane angle θ_y, which are expressed by Eq. (8):

$$\begin{cases} \left[\ddot{\theta}_x(t) + 2n\dot{\theta}_x(t)\right]\cos\theta_y(t) + 2\dfrac{\dot{l}(t)}{l(t)}\dot{\theta}_x(t)\cos\theta_y(t) - 2\dot{\theta}_x(t)\dot{\theta}_y(t)\sin\theta_y(t) \\ \qquad -\dfrac{1}{l(t)}\cos\theta_x(t)\left[\ddot{x}_p(t) + 2n\dot{x}_p(t)\right] \\ \qquad +\dfrac{1}{l(t)}\sin\theta_x(t)\left[\ddot{z}_p(t) + 2n\dot{z}_p(t)\right] + \dfrac{g}{l(t)}\sin\theta_x(t) = 0 \\ \ddot{\theta}_y(t) + 2\dfrac{\dot{l}(t)}{l(t)}\dot{\theta}_y(t) + \dot{\theta}_x^2(t)\sin\theta_y(t)\cos\theta_y(t) + \dfrac{1}{l(t)}\sin\theta_x(t)\sin\theta_y(t)\left[\ddot{x}_p(t) + 2n\dot{x}_p(t)\right] \\ \qquad +\dfrac{1}{l(t)}\cos\theta_y(t)\left[\ddot{y}_p(t) + 2n\dot{y}_p(t)\right] \\ \qquad +\dfrac{1}{l(t)}\sin\theta_y(t)\cos\theta_x(t)\left[\ddot{z}_p(t) + 2n\dot{z}_p(t)\right] + \dfrac{g}{l(t)}\sin\theta_y(t)\cos\theta_x(t) = 0 \end{cases}$$

(8)

In Eq. (8), $\left[x_p, y_p, z_p\right]$ are the coordinates of the hanging point P in the inertial coordinate system. g is the acceleration of gravity and l is the sling length.

In Eq. (8), the damping of the lifting load system is taken into account and a certain percentage of critical damping is acted on the lifted cargo. n is the damping coefficient. According to Michael (2000), damping ratio ξ is usually selected from 0.5% to 1% in order to determine the damping coefficient n. For the lifting load system, the damping coefficient n is:

$$n = \xi\sqrt{\frac{g}{l}} \tag{9}$$

In Eq. (9), g is the acceleration of gravity and l is the sling length.

III. THE FIRST PASSAGE FAILURE CRITERION

Introduced in this section is the first-passage failure criterion (also called the first passing), which is adopted to analyze the dynamic reliability of the lifting load system.

The structural dynamic responses (such as the stress and strain of the control point or the displacement of control layer, etc.) are regarded as random processes on the basis of the first-passage failure criterion. The structure is destroyed when its dynamic response firstly passes threshold b. The destruction when it is based on unilateral failure mode, is controlled by the random response $X(t)$. The dynamic reliability of this structure in time range [0, T] can be calculated with Eq. (10) (Li et al., 1993).

$$P_r(T) = P\left\{\left|X(t)\right| \le b, 0 < t \le T\right\} \tag{10}$$

In Eq. (10), b is the threshold of the random response $X(t)$ and $P_r(T)$ is the working safely probability of the structure.

The failure probability of the structure is:

$$P_f(T) = 1 - P_r(T) \tag{11}$$

In the Poisson process, the stationary random response $X(t)$ is assumed to be Gauss process of zero mean and the two arbitrarily intersections of the stationary random response $X(t)$ and the boundary are regarded as independent small probability event. According to the above hypothesis, the intersection numbers of the stationary random response $X(t)$ and the boundary in time range [0, T] are assumed to conform to the Poisson distribution. The stationary dynamic reliability of structures is expressed as in Eq. (12).

$$P_r(T) = \exp\left\{-\frac{1}{2\pi}\frac{\sigma_{\dot{X}}(t)}{\sigma_X(t)}T\exp\left[-\frac{b^2}{2\sigma_X^2(t)}\right]\right\} \tag{12}$$

In Eq. (12), b is the threshold of the random response $X(t)$.

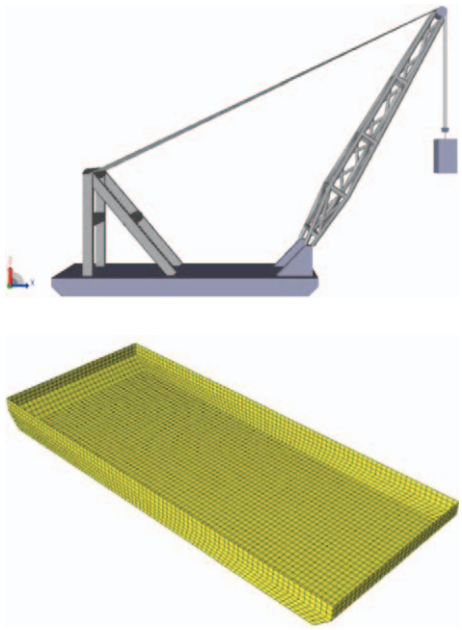

Fig. 3. The model of crane ship and its wet surface mesh.

T is effect time of random excitation

$\sigma_X(t)$ is the standard deviation of the random response $X(t)$.

$\sigma_{\dot{X}}(t)$ is the standard deviation of the random response $\dot{X}(t)$.

$$\sigma_X^2(t) = \int_0^\infty S_{XX}(\omega, t)d\omega \tag{13}$$

$$\sigma_{\dot{X}}^2(t) = \int_0^\infty \omega^2 S_{XX}(\omega, t)d\omega \tag{14}$$

$S_{XX}(\omega, t)$ is the self-power spectral density of the random response $X(t)$.

In this paper, the random response $X(t)$ is the angular displacement of the lifting load system: in-plane angle $\theta_x(t)$ and out-plane angle $\theta_y(t)$.

IV. CALCULATION MODEL AND PARAMETERS

The motion responses of a crane ship and its lifting load system are analyzed by numerical simulation in time domain and frequency domain with their motion equations. The model and parameters for numerical simulation are given in this section.

The model of crane ship and its wet surface mesh are shown in Fig. 3.

1. Main Parameters

Main dimensions of the crane ship are shown in Table 1.

The eigenvalues of the crane ship linear response obtained by frequency domain calculation are shown in the Table 2.

Table 1. Main dimensions of the crane ship.

Contents	Symbol	Value	Unit
Ship length	L	110	m
Ship width	B	46	m
Draft	D	2.75	m
Block coefficient	C_b	0.952	-
Displacement	Δ	13582.1	ton
Distance from center of gravity to baseline	x_g	0	m
	y_g	0	
	z_g	4	
Radius of gyration	k_{xx}	13.9	m
	k_{yy}	32.3	
	k_{zz}	35.1	
Coordinate of point *P* (related center of gravity)	x_p	120	m
	y_p	0	
	z_p	116	
Lift weight	M	1300	ton

Table 2. Eigenvalues of the crane ship.

	Natural period	Natural frequency
Heave	11.9	0.53
Roll	8.9	0.71
Pith	7.0	0.90

Table 3. Environment conditions.

	Water depth	Significant wave height Hs	Zero-crossing period Tz
Sea state one	200 m	0.1 m	5.8 s
Sea state two	200 m	0.5 m	7.0 s
Sea state three	200 m	1.0 m	7.8 s

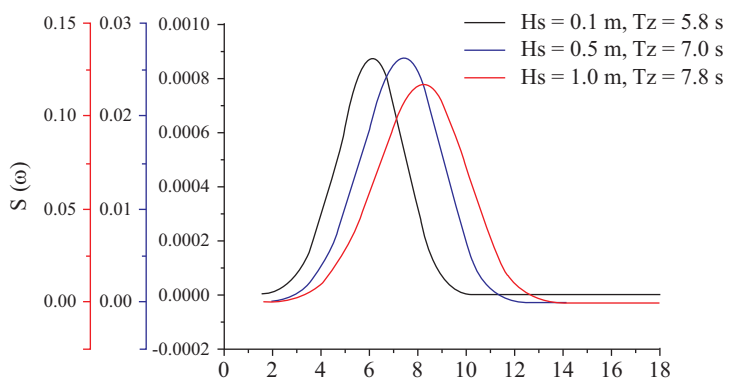

Fig. 4. Pierson-Moskowitz spectrum.

2. Wave Spectrum

How sea waves are caused by wind is a complicated process, so it is difficult to obtain a theoretical estimation of their spectrum by using the parameters of the wind. Currently, sea wave spectrums are derived from a great quantity of datum acquired from experience as well as by theoretical analysis.

In this paper, Pierson-Moskowitz spectrum is adopted as sea wave spectrum which is expressed in Eq. (15). P-M spectrum corresponding to the environmental conditions in Table 3 is shown in Fig. 4.

$$S(\omega) = \frac{a}{\omega^5} \exp\left(\frac{b}{\omega^4}\right) \tag{15}$$

Table 4. The maximum motion amplitudes of the crane ship.

	Hs = 0.1 m, Tz = 5.8 s		Hs = 0.5 m, Tz = 7.0 s		Hs = 1.0 m, Tz = 7.8 s	
Wave directions β	0°	30°	0°	30°	0°	30°
Surge (m)	0.005	0.004	0.037	0.033	0.082	0.077
Sway (m)	8.85e-9	0.004	7.55e-8	0.025	1.25e-6	0.066
Heave (m)	0.017	0.016	0.122	0.119	0.265	0.257
Roll (deg)	2.25e-8	0.018	3.61e-7	0.129	9.72e-6	0.374
Pith (deg)	0.016	0.014	0.114	0.097	0.245	0.205
Yaw (deg)	9.28e-9	0.007	7.96e-8	0.008	3.38e-6	0.103

Table 5. The maximum displacements of the lifted cargo for various sling lengths.

	In-plane angle (deg)		Out-plane angle (deg)		Displacement x (m)		Displacement y (m)		Displacement z (m)		Sling
Wave directions β	0°	30°	0°	30°	0°	30°	0°	30°	0°	30°	length (m)
Sea state one	0.05	0.04	5.6e-8	0.05	0.01	0.01	1.8e-8	0.01	0.05	0.04	50
	1.49	1.77	2.7e-6	1.7°	0.23	0.26	4.1e-7	0.27	0.05	0.05	8.35
Sea state two	0.33	0.26	3.8e-7	0.31	0.11	0.10	1.7e-7	0.09	0.35	0.32	50
	14.92	12.11	1.1e-5	10.19	3.20	2.60	2.6e-6	2.25	0.57	0.42	12.16
Sea state three	0.92	0.78	8.5e-7	0.60	0.42	0.38	5.1e-7	0.21	0.75	0.68	50
	29.24	29.59	3.2e-5	31.83	7.56	7.53	8.6e-6	7.96	2.30	2.71	15.10

In Eq. (15),

$$b = \left(\frac{2\pi}{T_z}\right)^4 \tag{16}$$

$$a = \frac{bH_s^2}{4} \tag{17}$$

In Eq. (16), T_z is zero-crossing period. In Eq. (17), H_s is significant wave height.

Elevation of irregular wave surface expressed by the wave spectrum is

$$\zeta(t) = \sum_{1}^{N} \sqrt{2S(\omega_j)\Delta\omega} \cdot \sin(\omega_j t + \varepsilon_j) \tag{18}$$

In Eq. (18), $S(\omega_j)$ is the power spectral density of sea wave and ω_j is the frequency of sea wave.

V. RESULTS AND DISCUSSION

In order to calculate responses of the lifting load system and parameters of these sea states, we adopt three levels of sea states to be environment conditions as in Table 3. For the calculation, the sling lengths are 50 m and the resonant length at different wave frequency. The wave directions are the head sea ($\beta = 0°$) and the first oblique waves ($\beta = 30°$). Random sea wave and random responses of the lifting load system are all assumed as stationary and various-state-included random process.

1. Maximum Responses of the Crane Ship and Its Lifting Load System

The responses of the crane ship and its lifting load system are calculated based on the second-order differential equations about in-plane and out-plane angle(shown in Eq. (8), the elevation equation of irregular wave surface (shown in Eq. (18)) and given conditions (shown in Tables 1-3) with time domain analysis method in this section. The maximum responses of the crane ship and its lifting system are shown in Tables 4 and 5 respectively.

The world famous ocean engineering company NOBLE DENTO requires, after many years of experience, that when the heave displacement of the lifted cargo reaches more than 0.75 m (Rawston et al., 1978), the workers should stop lifting work immediately and not restart until the sea environment conditions become better. By analyzing the calculation results in time domain, we find that the horizontal displacement of lifted cargo has reached meter-scale in sea state two (shown in Table 5), which will increase the dynamic tension of the sling and increase the collision opportunities between the lifted cargo and the crane ship. Therefore, Nojiri et al. (1983) demanded that the horizontal displacement of lifted cargo should not reach meter-scale.

In the sea state two, the thresholds of in-plane angle and out-plane angle are decided when the horizontal displacement of lifted cargo reaches meter-scale because the heave displacement of the lifted cargo in the sea state two is much smaller than 0.75 m. In the sea state three, the thresholds of in-plane angle and out-plane angle are decided when the heave displacement of the lifted cargo is larger than 0.75 m. In order to obtain the thresholds of

Table 6. The thresholds b of angular displacement.

		Sea wave direction β (deg)	Threshold b (deg)
Sea state two	in-plane angle θ_x	30°	4.3°
	out-plane angle θ_y	30°	5.2°
Sea state three	in-plane angle θ_x	30°	10.85°
	out-plane angle θ_y	30°	8.62°

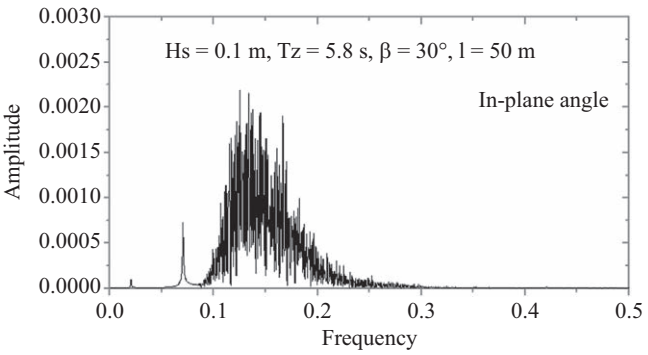

Fig. 5. Amplitude spectrum of cargo in-plane angle. Hs = 0.1 m, Tz = 5.8 s, *l* = 50 m.

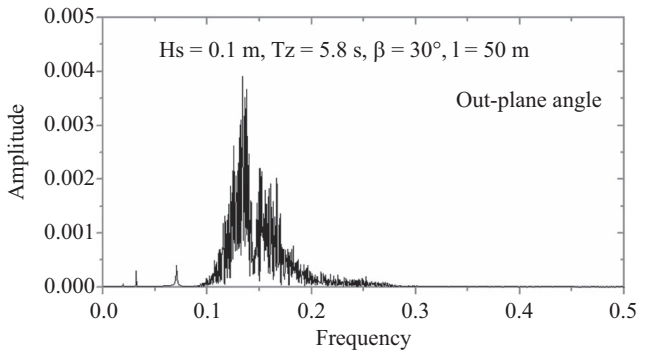

Fig. 6. Amplitude spectrum of cargo out-plane angle. Hs = 0.1 m, Tz = 5.8 s, *l* = 50 m.

in-plane angle and out-plane angle in different sea states, we do the following work. Firstly, we calculate the displacement of the crane ship in time domain (shown in Table 4). Secondly, we calculate the space displacements of lifted cargo (shown in Table 5). Lastly, we decide the thresholds b of in-plane angle and out-plane angle with Eq. (4) and Eq. (5) (shown in Table 6) on the basis of these calculations.

2. Angular Displacement Response Spectrum of the Lifted Cargo with Different Sling Lengths and the First Oblique Waves (β = 30°) in Different Sea States.

In this section, by using spectrum analysis, we calculate the response spectrums of the lifting load system of the crane ship and our calculation is based on the second-order differential equations about in-plane and out-plane angle (shown in Eq. (8)), Pierson-Moskowitz spectrum (shown in Eq. (15)) and the given conditions in Tables 1-3. Angular displacement response spectrums of the lifted cargo are shown in Figs. 5-16. Frequency

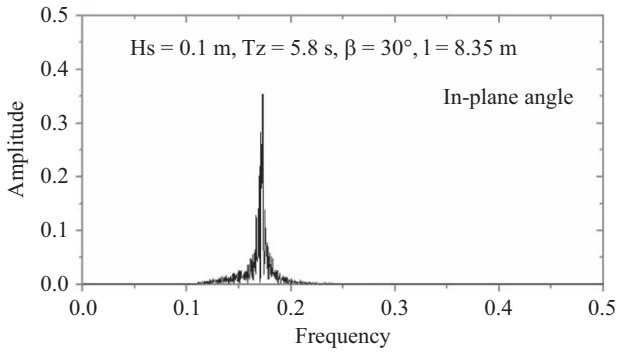

Fig. 7. Amplitude spectrum of cargo in-plane angle. Hs = 0.1 m, Tz = 5.8 s, *l* = 8.35 m.

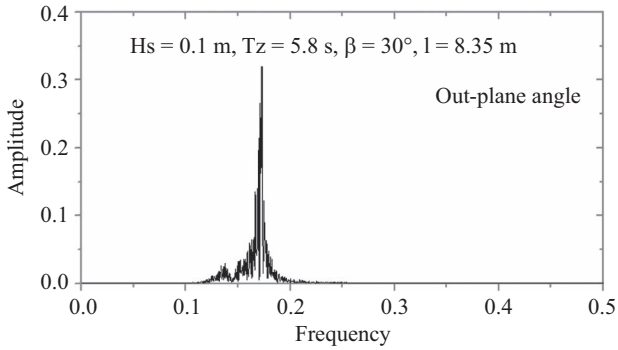

Fig. 8. Amplitude spectrum of cargo out-plane angle. Hs = 0.1 m, Tz = 5.8 s, *l* = 8.35 m.

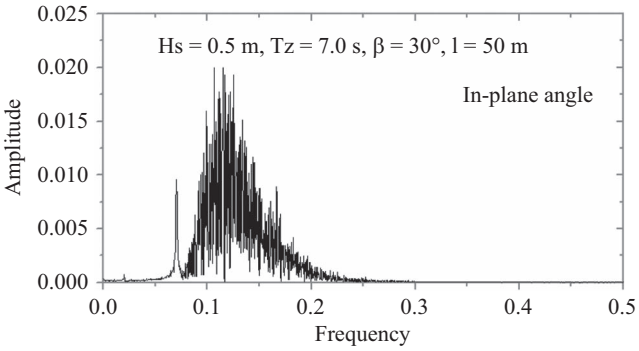

Fig. 9. Amplitude spectrum of cargo in-plane angle. Hs = 0.5 m, Tz = 7.0 s, *l* = 50 m.

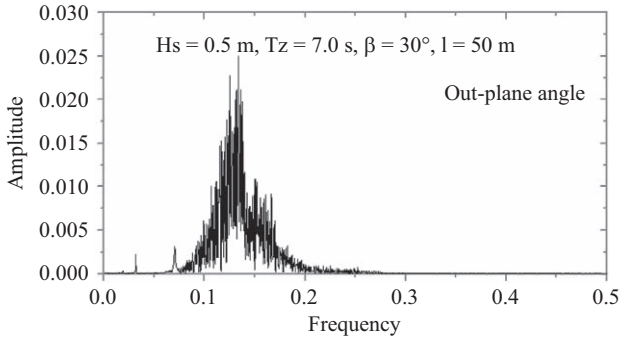

Fig. 10. Amplitude spectrum of cargo out-plane angle. Hs = 0.5 m, Tz = 7.0 s, *l* = 50 m.

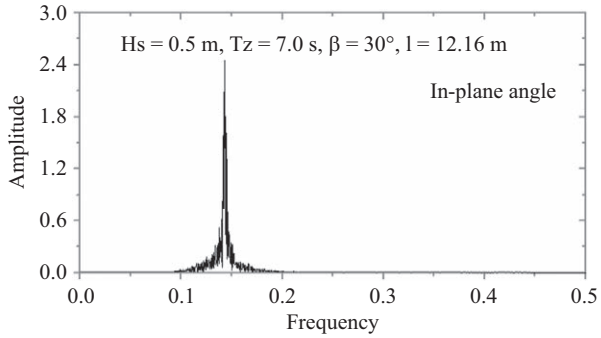

Fig. 11. Amplitude spectrum of cargo in-plane angle. Hs = 0.5 m, Tz = 7.0 s, *l* = 12.16 m.

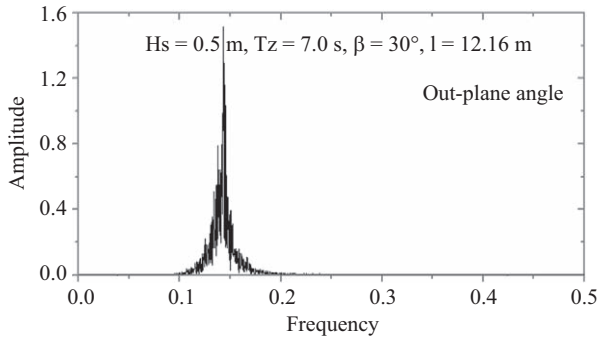

Fig. 12. Amplitude spectrum of cargo out-plane angle. Hs = 0.5 m, Tz = 7.0 s, l = 12.16 m.

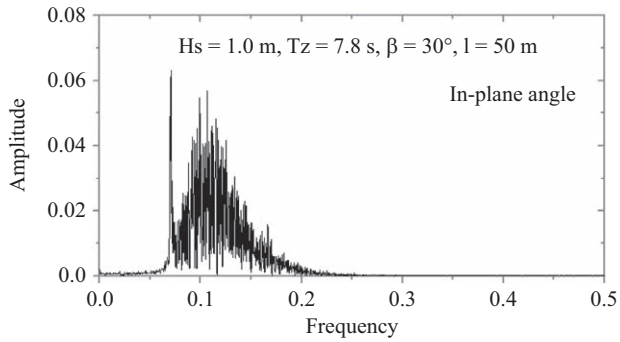

Fig. 13. Amplitude spectrum of cargo in-plane angle. Hs = 1.0 m, Tz = 7.8 s, *l* = 50 m.

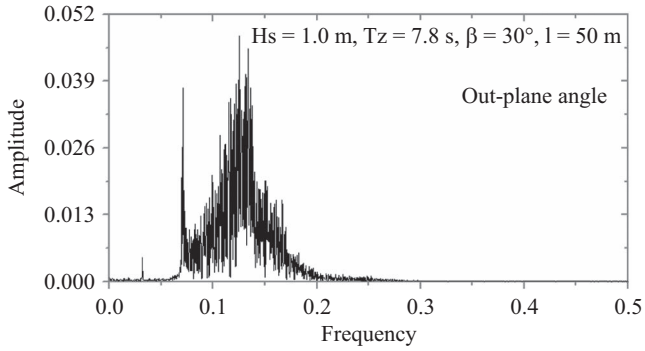

Fig. 14. Amplitude spectrum of cargo out-plane angle. Hs = 1.0 m, Tz = 7.8 s, *l* = 50 m.

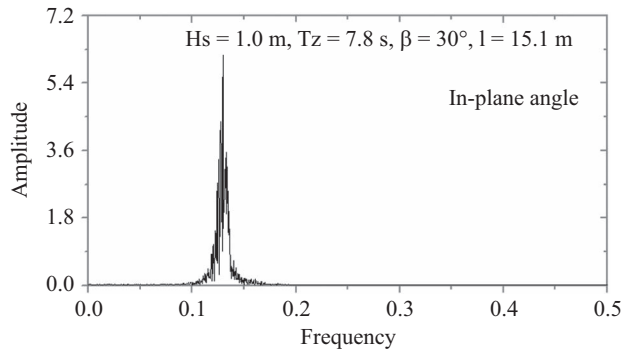

Fig. 15. Amplitude spectrum of cargo in-plane angle. Hs = 1.0 m, Tz = 7.8 s, *l* = 15.1 m.

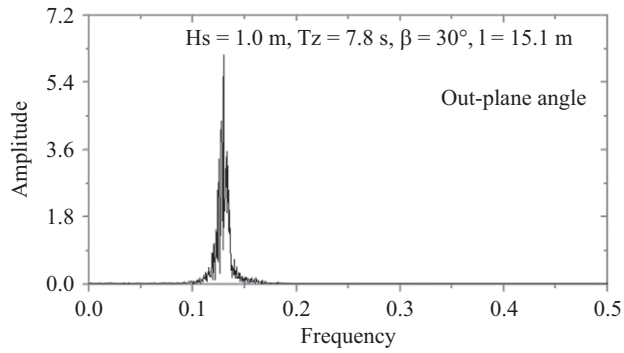

Fig. 16. Amplitude spectrum of cargo out-plane angle. Hs = 1.0 m, Tz = 7.8 s, *l* = 15.1 m

unit is Hz and the amplitude unit of self-power spectral density $S_{XX}(\omega, t)$ is $(\text{rad})^2 \cdot \text{s}$ in these figures.

It can be found from Fig. 5 to Fig. 16 that in the three sea states when the sling length is 50m, the angular displacement spectrum values $S_{XX}(\omega, t)$ of the lifted cargo is very small and it is impossible for its displacements to reach the boundary conditions, so the analysis of the dynamic reliabilities of the lifting load system becomes unnecessary. The time domain analysis shows that in the sea state one, when the sling length is a resonance one, the angular displacement spectrum values of lifted

Table 7. Variances of angular displacement and angular velocity.

		Sea wave direction β (deg)	Variance of angular displacement $\sigma_X^2(t)(\mathrm{rad})^2$	Variance of angular speed $\sigma_{\dot{X}}^2(t)(\mathrm{rad/s})^2$
Sea state two	in-plane angle θ_x	30°	52.2440	1.4165
	out-plane angle θ_y	30°	50.5561	1.5242
Sea state three	in-plane angle θ_x	30°	152.1570	4.0157
	out-plane angle θ_y	30°	126.6926	2.1659

Table 8. Dynamic reliability analysis results.

		Sea wave direction β (deg)	Effect time of sea wave *T*(*s*)	Threshold b (deg)	Variance of angular displacement $\sigma_X^2(t)(\mathrm{rad})^2$	Variance of angular speed $\sigma_{\dot{X}}^2(t)(\mathrm{rad/s})^2$	Dynamic reliability
Sea state two	in-plane angle θ_x	30°	8.4	4.3°	52.2440	1.4165	0.8316
	out-plane angle θ_y	30°	8.4	5.2°	50.5561	1.5242	0.8372
Sea state three	in-plane angle θ_x	30°	9.36	10.85°	152.1570	4.0157	0.8484
	out-plane angle θ_y	30°	9.36	8.62°	126.6926	2.1659	0.8648

cargo is also smaller and the displacements of the crane ship are very small (shown in Table 4). Therefore, in the sea state one when the sling length is resonance one, it is impossible for the displacements of the lifted cargo reach the boundary conditions and the dynamic reliabilities analysis of the lifting load system in this situation becomes unnecessary. In the sea state two and the sea state three when the sling length is resonance one, the angular displacement spectrum values of the lifted cargo increase quickly, so the dynamic reliabilities of lifted cargo are analyzed in this paper.

Variances of angular displacement and angular velocity about the in-plane angle and out-plane angle can be calculated based on Eq. (13), Eq. (14) and their self-power spectral density $S_{XX}(\omega, t)$ (shown in Fig. 5 to Fig. 16). The calculation results are shown in Table 7.

3. Results of Dynamic Reliability Analysis

The dynamic reliability of the lifting load system are calculated with the dynamic reliability calculation formula based on the first-passage failure criterion(shown in Eq. (12)), the thresholds b of angular displacement(shown in Table 6) and the variances of angular displacement and angular velocity (shown in Table 7). The effect time of the sea wave is calculated based on Eq. (19). The calculation results are shown in Table 8.

The effect time of the sea wave T is obtained from the characteristic period of the sea wave,

$$T = 1.2T_z \tag{19}$$

In Eq. (19), T_z is the zero-crossing period of sea wave.

When analyzing the dynamic reliability of the lifted cargo, we find that when the sling length is resonance one, the significant wave height of sea state two is as small as 0.5 m while the maximum horizontal displacements of the lifted cargo are as large as (direction x and direction y) 3.20 m and 2.25 m respectively. In addition, the probabilities that the horizontal displacement of lifted cargo don't reach to meter-scale are 0.8316 corresponding in-plane angle and 0.8372 corresponding out-plane angle in resonance area. According to the above mentioned analysis results, despite the small significant wave height, the resonance responses in the sea state two are too large to carry out the lifting work. Therefore, we should select the proper length of the sling so that the resonance area can be avoided.

When the significant wave height of the sea state three reaches 1.0 m, the horizontal displacements of crane ship exceeds 1.0 m. As a result, to ensure the safety of the lifting work, it is necessary to reduce the displacements of the crane ship (like increasing the mooring line pre-tension). In sea state three, the thresholds of in-plane angle and out-plane angle are decided on the condition that the lifted cargo heave displacement isn't larger than 0.75 m. In resonance area of the sea state three, the probability of the lifted cargo heave displacement being no larger than 0.75 m is 0.8488 for the in-plane angle and 0.8648 for the out-plane angle. These analysis results illustrate that the sea state three is high sea state, its sea wave height exerts obvious effects on the motions of the crane ship and the lifted cargo, and the probability of the lifted cargo heave displacement being larger than 0.75 m isn't small and is almost 15% in the resonance area. As is mentioned above, the world famous ocean engineering company NOBLE DENTO requires that the heave displacement of the lifted cargo should not be larger than 0.75 m, otherwise the workers must stop lifting work, so it is necessary to take measures to avoid the resonance area in the sea state three.

VI. CONCLUSIONS

(1) We must evaluate the dynamic reliability of the crane ship lifting load system so as to obtain the probability of the lifting load system working safely under the given sea states, but there are no literatures mentioning its dynamic reliability analysis based on reliability evaluation. In this paper, the dynamic reliability evaluation method of the crane ship lifting load system is explored and the probability of lifting load system working safely under the given sea states is calculated. In this paper, we adopt three levels of sea states to be environment conditions, which are sea state one, sea state two, sea state three. Lifting work on a crane ship is permitted under these sea states according to international standards. By analyzing and calculating, we find that the dynamic responses of the lifting load system and the crane ship in the resonance area are much more than ones in the off-resonance area. The dynamic reliability analysis of the crane ship lifting load system results that the probability of lifting load system working safely under sea state two and sea state two is almost 85% , so it is necessary to adopt a measure to avoid the resonance area in order to the lifting load system working safely.

(2) The confirmation criterions of the thresholds are given. The thresholds of in-plane angle and out-plane angle are decided according to the horizontal displacement of lifted cargo not to reach meter-scale in the sea state two. The thresholds of in-plane angle and out-plane angle are decided according to the heave displacement of the lifted cargo not to be larger than 0.75 m in the sea state three.

(3) According to the response spectrums of the crane ship lifting load system calculated by using spectrum analysis, the angular displacement spectrum values $S_{XX}(\omega, t)$ of the lifted cargo are all very small in the three sea states when the lifting load system is far away from the resonance area , so their dynamic reliabilities of the lifting load system need not be analyzed. Because the significant wave height of the sea state one is only 0.1 m, the angular displacement spectrum values of the lifted cargo is also very small in the resonance area and the dynamic reliabilities of the lifting load system in this condition also need not be analyzed.

(4) In the resonance area of the sea state two , the horizontal displacements of lifted cargo are large (the maximum horizontal displacements of the lifted cargo are as large as (direction x and direction y) 3.20 m and 2.25 m respectively.) and the probabilities that the horizontal displacement of lifted cargo don't reach to meter-scale are 0.8316 corresponding in-plane angle and 0.8372 corresponding out-plane angle, so it is necessary that adjusting the sling length to avoid the resonance area, although significant wave height of the sea state two is small (the significant wave height of sea state two is 0.5 m).

(5) The sea state three is high sea state, and its sea wave height (1.0 m) exerts obvious effects on the motions of the crane ship and the lifted cargo. The horizontal displacement of crane ship have exceeded one meter, therefore it is necessary that adopting a measure to reduce displacements of the crane ship in order to ensure the safety of the lifting work. (like increasing mooring line pre-tension).

(6) In the resonance area of the sea state three , the probabilities that heave displacement of the lifted cargo isn't larger than 0.75 m are 0.8488 for in-plane angle and 0.8648 for out-plane angle, so the probability of the lifted cargo heave displacement being larger than 0.75 m isn't small and is almost 15% in the resonance area. NOBLE DENTO, the world famous ocean engineering company, requires that the heave displacement of the lifted cargo can't be bigger than 0.75 m, otherwise the workers must stop the lifting work, so it is necessary to adopt measure to avoid the resonance area in the sea state three.

REFERENCES

Al-Sweiti, Y. M. and D. Sŏffker (2007). Planar cargo control of elastic ship cranes with the "Maryland rigging" system. Journal of Vibration and Control Series 3, 241-267.

Balachandran, B., Y.-Y. Li and C.-C. Fang (1999). A mechanical filter concept for control of non-linear crane load oscillations. Journal of Sound and Vibration Series 3, 651–682.

Becker ,G., L. Camarinopoulos and D. Kabranis (2002). Dynamic reliability under random shocks. Reliability Engineering and System Safety Series 3, 239-251.

Cha, J. H., I. M. Roh and Y. K. Lee (2010). Dynamic response simulation of a heavy cargo suspended by a floating crane based on multibody system dynamics. Journal Ocean Engineering Series 37, 1273-1291.

Chaudhuri, A. and S. Charkraborty (2006). Reliability of linear structures with parameter uncertainty under non-stationary earthquake. Structural Safety Series 3, 231-246.

Chen, L., C. Zhang and X. Y. Zhang (2011). The response of large crane ship to waves. Journal of Shanghai Ship and Shipping Research Institute Series 2, 299-102.

Chin, C. M., A. H. Nayfeh and D. T. Mook (2001). Dynamics and control of ship-mounted cranes. Journal of Vibration and Control September Series 6,891-904.

Clauss, G. and T. Riekert (1992). Influence of load motion control on the operational limitations of large crane vessels in severe environment. Proceedings International Conference on Behaviour of Offshore Structures. BPP Technical Services, Pergamon, Oxford, England, 1112-1125.

Ellermann, K., E. Kreuzer and M. Markiewicz (2002). Nonlinear dynamics of floating cranes. Nonlinear Dynamics Series 2, 107-183.

Fritz, C., H. Gerhard and K. Wolfgang (1995). Dynamic reliability of nonlinear systems under random excitation. American Society of Mechanical Engineers Series 3, 1007-1024.

Gasparini, D. A. (1979). Response of MDOF systems to non-stationary random excitation. Journal of the Engineering Mechanics Division Series 1, 13-18.

Harnett, M. (2000). The application of a spectral response model to fixed offshore structures. Compeers and Structures Series 78, 355-364.

Henry, R. J., Z. N. Masoud, A. H. Nayfeh and D. T. Mook (2001). Cargo pendulation reduction on ship-mounted cranes via boom-luff angle actuation. Journal of Vibration and Control Series 8, 1253-1264.

Iwan, W. D. and N. C. Gates (1979). Estimations earthquake response of simple hysteretic structures. Journal of Applied Mechanics Series 46, 391-405.

Iwan, W. D. and P. T. Spanos (1978). Response envelope statistics for nonlinear oscillators with random excitation. Journal of Applied Mechanics Series 45, 170-174.

Iyenger, R. N. (1973). First passage probability during random vibration. Journal of Sound and Vibration Series 2, 185-193.

Kaplunov, J. D., E. V. Nolde and B. F. Shorr (2005). A perturbation approach for evaluating natural frequencies of moderately thick elliptic plates. Journal of Sound and Vibration Series (3-5), 905-919.

Kral, R., E. Kreuzer and C. Wilmers (1995). Nonlinear oscillations of a crane ship. Proceedings of the 3rd International Conference on Industrial and Applied Mathematics, Hamburg, Germany, Suppl 4, 5-8.

Li, D. X. (2002). Advanced structural dynamics. science press, Beijing, China.

Li, G., H. Cao, Q. Li and D. Huo (1993). Structural dynamic reliability theory and application. Seismological Press, Beijing, China.

Mahadevan, S. and S. Mehta (1993). Dynamic reliability of large frames. Computers and Structures Series 1, 57-67.

Masoud, Z. N., A. H. Nayfeh and D. T. Mook (2004). Cargo pendulation reduction of ship-mounted cranes. Journal Nonlinear Dynamics Series 35, 299-311.

Mochio, T. (1989). Dynamic reliability of hysteretic structures under combined random Loads. JSME International Journal, Series 3: Vibration, Control Engineering, Engineering for Industry Series 1, 19-24.

Mochio, T. (1989). Dynamic reliability of multi-degrees-of-freedom structures with hysteretic characteristics under combined random loads. Proceedings of ICOSSAR '89, the 5th International Conference on Structural Safety and Reliability, San Francisco, America, 1363-1370.

Nojiri, N. and T. Sasaki (1983). Motion Characteristics of Crane Vessels in Lifting Operation. Proceedings of the 15th Annual Offshore Technology Conference, Houston, Texas, America, 4603.

Patel, M. H., D. T. Brown and J. A. Witz (1987). Operability analysis for a monohull crane vessel. Naval Engineering Journal Series 3, 256-263.

Rawston, P. J. and G. J. Blight (1978). Prediction of Weather Downtime for Derrick Barges. Proceedings of the 10th Annual Offshore Technology Conference, Houston, Texas, America, 3150.

Ren, H. L., X. Wang, Y. J. Hu and C. G. Li (2008). Dynamic response analysis of a moored crane-ship with a flexible boom. Journal of Zhejiang University Science A Series 1, 26-31.

Rice, S. O. (1944). Mathematical analysis of random noise. Bell System Technical Journal Series 23,282-332.

Roberts, J. B. (1975). Probability of first-passage failure for non-stationary random vibration. Journal of Applied Mechanics Series 42, 716-720.

Roberts, J. B. (1978a). First passage time for oscillators with non-linear damping. Journal of Applied Mechanics Series 45, 175-180.

Roberts, J. B. (1978b). The energy envelope of a randomly excited non-linear oscillator. Journal of Sound and Vibration Series 2, 177-185.

Schellin, T. E., T. Jiang and S. D. Sharma (1991). Crane ship response to wave groups. Journal of Offshore Mechanics and Arctic Engineering Series 113, 211-218.

Van den Nieuwenhof, B. and J. P. Coyette (2003). Modal approaches for the stochastic finite element analysis of structures with material and geometric uncertainties. Computer Methods in Applied Mechanics and Engineering Series (33-34), 3705-3729.

Vaughers,T. and M. Mardiros (1997). Joint logistics over the shore operations in rough seas. Naval Engineering Journal Series 109(3), 385-393.

Yang, J. N. and M. Shinozuka (1971). On the first excursion probability in stationary narrow band random vibration. Journal of Applied Mechanics Series 38, 1017-1022.